Life Sciences 239 (2019) 117070

Contents lists available at ScienceDirect

Life Sciences

journal homepage: www.elsevier.com/locate/lifescie

Neonatal murine engineered cardiac tissue toxicology model: Impact of dexrazoxane on doxorubicin induced injury

Juan Zhen[a,b], Haitao Yu[a,b], Honglei Ji[a], Lu Cai[b,c,d], Jiyan Leng[a,*], Bradley B. Keller[d,e,**]

[a] The First Hospital of Jilin University, Changchun 130021, China
[b] The Pediatric Research Institute, Department of Pediatrics, the University of Louisville School of Medicine, Louisville, KY 40292, USA
[c] Department of Radiation Oncology, the University of Louisville School of Medicine, Louisville, KY, USA
[d] Department of Pharmacology and Toxicology, University of Louisville, Louisville, KY 40202, USA
[e] Kosair Charities Pediatric Heart Research Program, Cardiovascular Innovation Institute, University of Louisville School of Medicine, Louisville, KY 40202, USA

ARTICLE INFO

Keywords:
Cardiotoxicity
Dexrazoxane
Doxorubicin
Engineered cardiac tissue
Metallothionein
Topoisomerase 2B
Zinc

ABSTRACT

Doxorubicin (DOX) induced cardiotoxicity is a life-threatening side effect of chemotherapy and decreased cardiac function can present years after treatment. Despite the investigation of a broad range of pharmacologic interventions, to date the only drug shown to reduce DOX-related cardiotoxicity in preclinical studies and limited clinical trials is the iron chelating agent, dexrazoxane (DRZ), although the mechanisms responsible for DRZ mediated protection from DOX related cardiotoxicity remain unclear. Engineered cardiac tissues (ECTs) can be used for tissue repair strategies and as in vitro surrogate models to test cardiac toxicities and preventative countermeasures. Neonatal murine ECTs display cardiotoxicity in response to the environmental toxin, cadmium, and reduced cadmium toxicity with Zinc co-treatment, in part via the induction of the anti-oxidant Metallothionein (MT). We adapted our in vitro ECT model to determine the feasibility of using the ECT approach to investigate DOX-related cardiac injury and DRZ prevention. We found: (1) DOX induced dose and time dependent cell death in ECTs; (2) Zinc did not show protection from DOX cardiotoxicity; (3) MT overexpression induced by Zinc, low dose Cd pretreatment, or MT-overexpression (MT-TG) did not reduce ECT DOX cardiotoxicity; (4) DRZ reduced ECT DOX induced cell death; and (5) The mechanism of DRZ ECT protection from DOX cardiotoxicity was topoisomerase 2B (TOP2B) inhibition rather than reduced reactive oxygen species. Our data support the feasibility of ECTs as an in vitro platform technology for the investigation of drug induced cardiotoxicities including the role of TOP2B in DOX toxicity and DRZ mediated DOX toxicity prevention.

1. Introduction

Over the past 20 years 3-dimensional (3D) ECTs have proven to be a robust in vitro platform technology for drug screening [1–63], tissue repair [2–4], human genetic disease modeling and repair [5–8], and recently, environmental toxicity [9]. 3D ECTs have multiple advantages over traditional single cell or monolayer (two-dimensional) culture methods including the formation of isotropic and aligned myocardial tissues that are electrically and mechanically and function similar to in vivo myocardium [3,5,10], the ability to customize cell composition to include multiple mesoderm lineages and/or genetically altered cells [3,5], and the ability to scale up ECT platforms for drug testing [11,12].

Doxorubicin (DOX), is an anthracycline antibiotic and a topoisomerase II (TOP2)-targeting drug and is frequently used in chemotherapy protocols. However, DOX treatment is associated with late-presenting and progressive cardiotoxicity associated with significant morbidity and mortality [13–17], is of particular risk for pediatric cancer patients [18], and may have genetic associations [19–21]. Due to the clinical effectiveness of DOX in chemotherapeutic protocols for children and adults, multiple strategies have been investigated to reduce DOX cardiotoxicity.

While limiting the total DOX dose has been shown to reduce the incidence of cardiotoxicity, pre-clinical investigations of medications that might prevent DOX induced cardiac injury [22–24] have largely failed to prevent DOX cardiotoxicity in clinical trials [25]. DOX cardiotoxicity is mediated, in part, through altered calcium signaling [26,27], mitochondrial iron accumulation [28] and injury [29] which increases ROS levels [30], and autophagy [31,32]. Epigenetic variants

* Correspondence to: J. Leng, the First Hospital of Jilin University, 71 Xinmin Street, Changchun 130021, China.
** Correspondence to: B. B. Keller, Kosair Charities Pediatric Heart Research Program, Cardiovascular Innovation Institute, University of Louisville School of Medicine, Louisville, KY 40202, USA.
E-mail addresses: jiyanleng2013@163.com (J. Leng), Brad.Keller@louisville.edu (B.B. Keller).

https://doi.org/10.1016/j.lfs.2019.117070
Received 16 August 2019; Received in revised form 28 October 2019; Accepted 14 November 2019
Available online 18 November 2019
0024-3205/

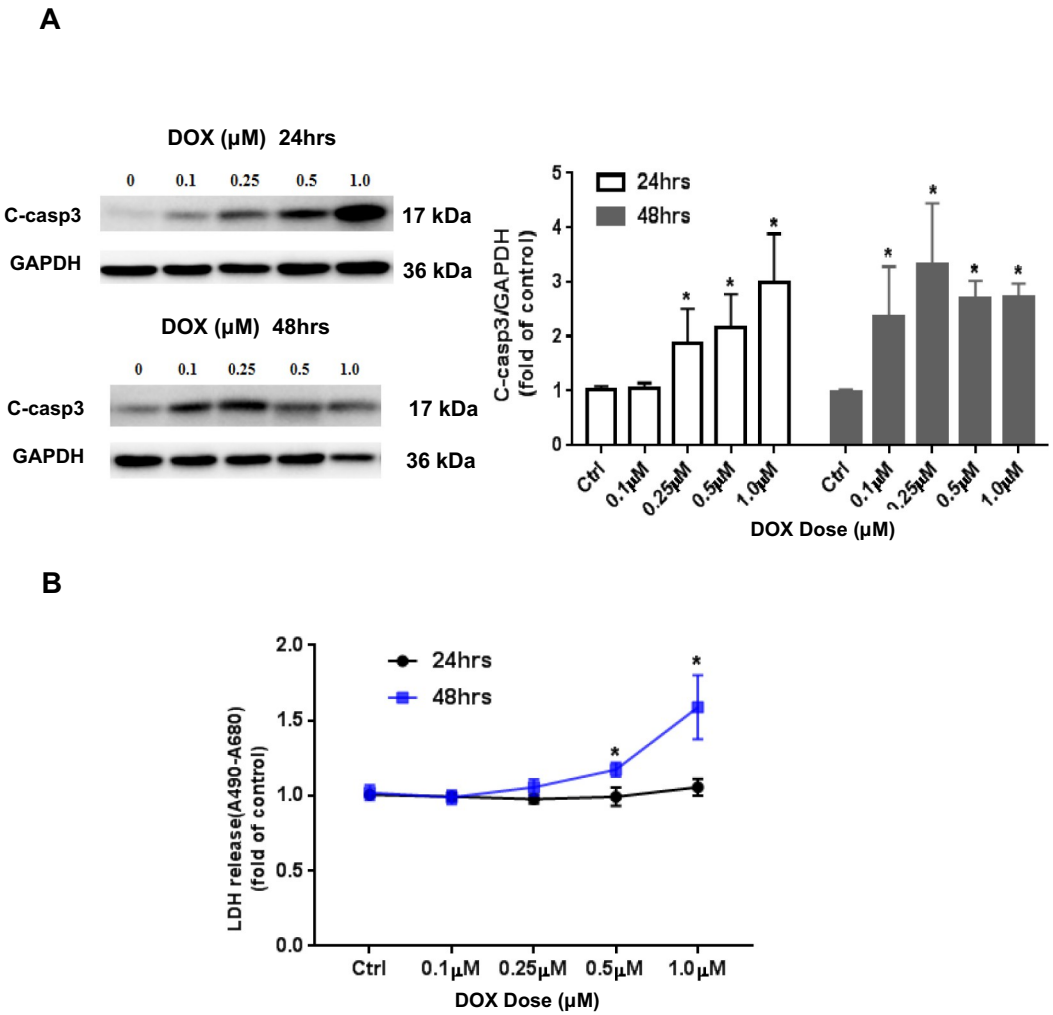

Fig. 1. Dose and time response of toxic DOX effect on murine ECTs. A, Expression of Cleaved caspase-3 after DOX treatment (0 μM; 0.1 μM; 0.25 μM; 0.5 μM; 1.0 μM) for 24 h and for 48 h; $n = 3$ to $n = 5$ ECT per group per time point. B, LDH release after increasing DOX treatment (0 μM; 0.1 μM; 0.25 μM; 0.5 μM; 1.0 μM) for 24 h and for 48 h; n = 3 to n = 5 ECT per group per time point. *$P < .05$ vs. corresponding normalized Ctrl.

Table 1
Dose and time dependent DOX effect on inhibition of ECT beating. ECT beating was recorded for 15 s following increasing DOX dose (0 μM; 0.1 μM; 0.25 μM; 0.5 μM; 1.0 μM) and exposure (12 h, 24 h, 36 h, 48 h, 60 h and 72 h). Percentage of ECTs with absent beating are displayed, n = 4 to 9 ECT per group.

DOX	12 h	24 h	36 h	48 h	60 h	72 h
0.0 μM (n = 4)	0	0	0	0	0	0
0.1 μM (n = 4)	0	0	0	0	0	0
0.25 μM (n = 6)	0	0	0	0	0	33.3%
0.5 μM (n = 9)	0	0	11.1%	88.9%	88.9%	100%
1.0 μM (n = 7)	0	85.7%	100%	100%	100%	100%

that increase tolerance for oxidative stress may reduce DOX effectiveness [33,34]. Zinc has been shown in limited preclinical studies to reduce DOX induced cardiomyocytes injury via the induction of Nrf2 [35], as has the anti-oxidant Metallothionein (MT) [36,37] where MT overexpression reduces DOX cardiotoxicity in vitro [38] and in vivo [39]. The antioxidant flavonoid Apigenin has also been shown to reduce DOX cardiotoxicity in rats [40]. Currently, dexrazoxane (DRZ) is the only clinically indicated drug used to protect against DOX cardiotoxicity [41,42]. The mechanism for the protection has been primarily attributed to iron chelation by the EDTA-like hydrolysis of DRZ, which decreases hydroxyl free radicals [43], inhibits Topoisomerase 2B (TOP2B) mediated DNA double-strand breaks [19,44], and reduces mitochondrial injury [45].

In the current study we tested the hypothesis that in vitro murine ECT can rapidly display DOX mediated cardiomyocyte injury and can be used to investigate the protective effect of DRZ to reduce DOX toxicity. ECTs displayed rapid and reproducible DOX mediated cardiotoxicity, no effect of supplemental Zinc to reduce toxicity, and the ability of DRZ to prevent Dox cardiotoxicity. The DRZ protective effect occurred via TOP2B inhibition rather than changes in ROS. Thus, neonatal murine ECTs may be a robust and rapid in vitro model to screen additional compounds with the potential to reduce DOX toxicity prior to preclinical, in vivo validation.

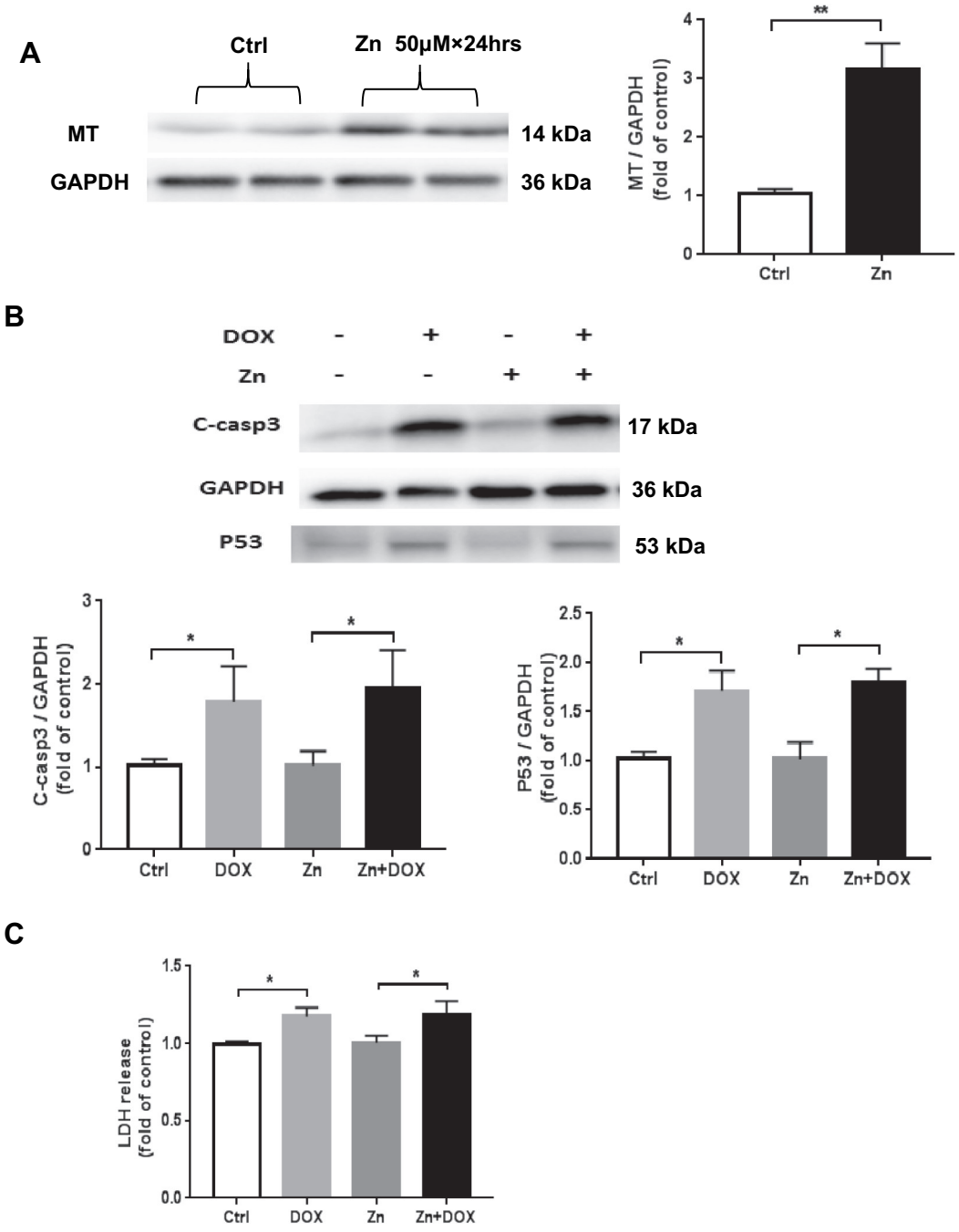

Fig. 2. Zinc induced MT but did not reduce ECT DOX toxicity. A, Zinc (50 μM for 24 h) induced MT expression. n = 3 ECT per group. B, Cleaved caspase-3 expression increased after DOX (0.5 μM for 24 h) and was not reduced by Zinc pretreatment (50 μM for 2 h prior to DOX treatment) and Zinc treatment did not alter baseline cleaved caspase-3. n = 4 to 8 ECT per group. C, Similar to cleaved caspase-3, LDH release increased after DOX (0.5 μM for 24 h) and was not reduced by Zinc pretreatment (50 μM for 2 h prior to DOX treatment) and Zinc treatment did not alter baseline LDH release. n = 4 to 10 ECT per group; $^{*}P < .05$ and $^{**}P < .01$ vs. Ctrl ECT.

2. Materials and methods

2.1. Animals: neonatal wild type and MT-TG mice

Cardiac-specific MT gene overexpressing transgenic (MT-TG) mice were produced from FVB wild-type (WT) mice obtained from Harlan Bioproducts for Science (Indianapolis, IN) as used in previous studies [9,46]. Both MT-TG and WT mice were housed in the University of Louisville Research Resources Center at 22 °C with a 12-hrs light/dark cycle and were provided free access to standard rodent chow and tap

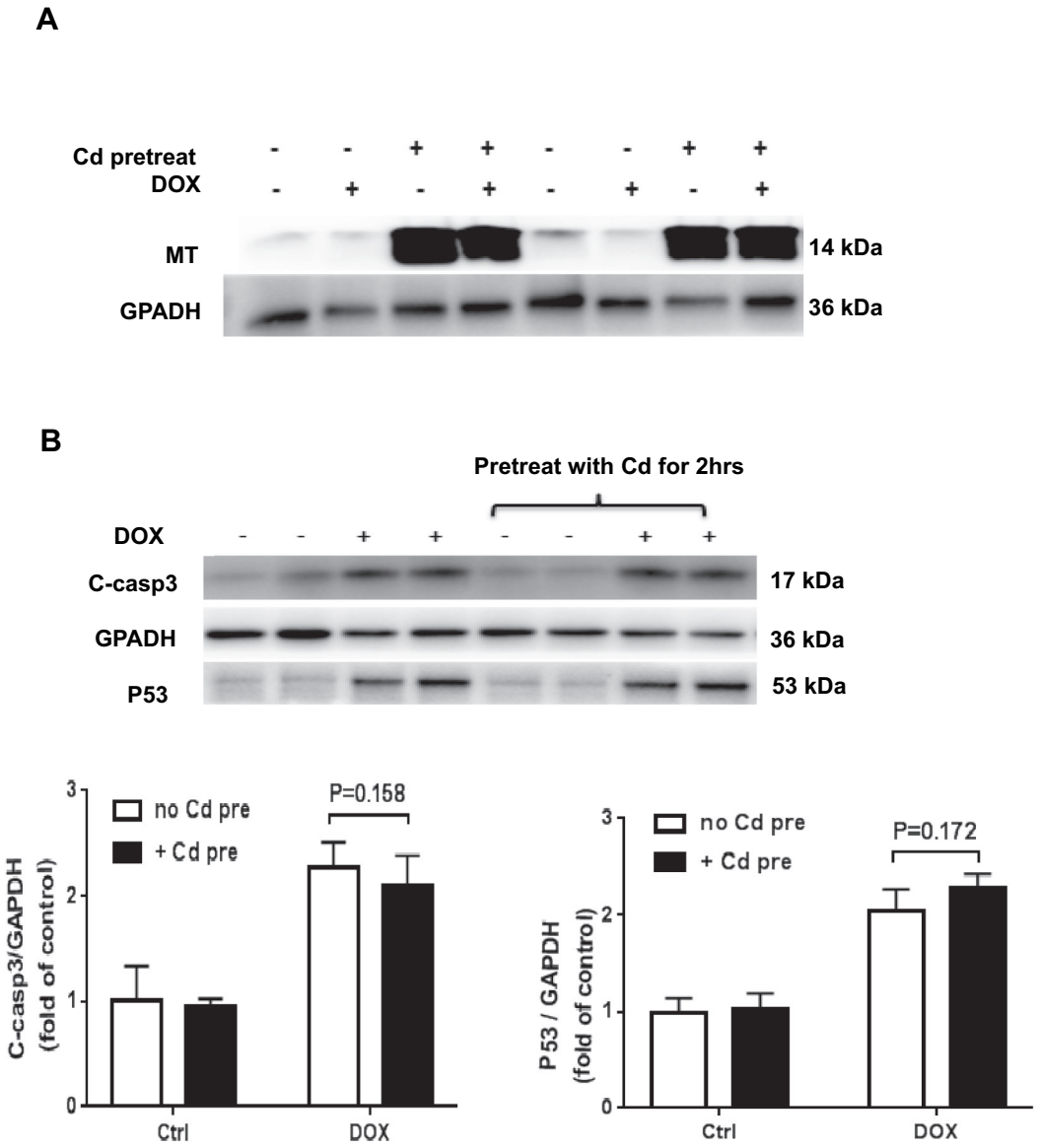

Fig. 3. Cadmium pretreatment did not reduce ECT DOX toxicity. A, Cd pretreatment (5 μM for 2 h), but not DOX treatment (0.5 μM for 24 h), induced MT. B, Cd pretreatment (5 μM for 2 h), but not reduce DOX (0.5 μM for 24 h) induced increased cleaved caspase-3 and P53 expression. n = 3 to 5 ECT per group.

water. All animal procedures were approved by the Institutional Animal Case and Use Committee, which is certified by the American Association for Accreditation of Laboratory Animal Care. We bred FVB and MT-TG mice to generate FVB and MT-TG pups, respectively, in order to generate WT- and MT-TG-ECTs.

2.2. Isolation of neonatal mouse ventricular cardiac cells

Neonatal mouse ventricular cardiac cells were isolated as previous described [9]. Briefly, hearts of 3-day-old pups were harvested and digested by trypsin and collagenase. CM were enriched by preplating for 45 min followed by rotating for 4 h and then heart cells were collected and counted using a hemocytometer.

2.3. ECT construction and treatment

ECTs were constructed as previous described [5,9]. Approximately 0.8×10^6 heart cells derived from 4 pup ventricles were mixed with collagen and matrigel, poured to form a cylinder construct within Flexcell Tissue TrainTM culture plates (Flexcell International), and incubated for 2 h (37 °C, 5% CO_2) to form a cylindrical ECT construct. Following initial ECT gelation, 4 mL of mouse medium was added to each ECT in the 6-well culture dish. ECTs were maintained in vitro for 7 days with media changes every other day. Starting on day 6, ECTs were pretreated with Zinc (50 μM/L), NAC (1 mM/L), Cadmium (5 μM/L) or DRZ (1 μM/L) for 2 h followed by treatment with 0.5 μmol/L DOX for another 24 h. Control ECTs were treated with standard media. DRZ, NAC, and DOX were purchased from Sigma.

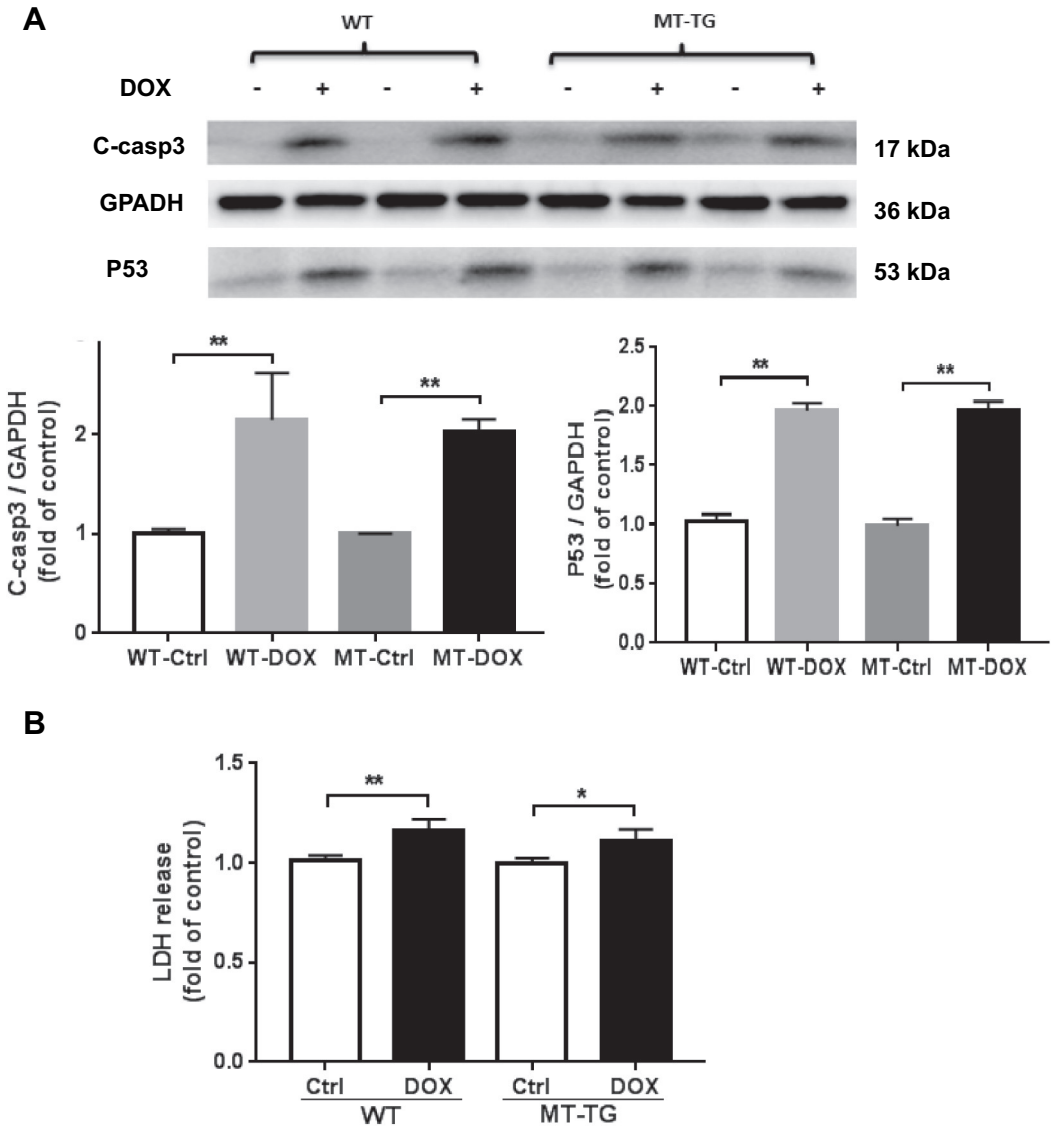

Fig. 4. MT overexpression did not reduce ECT DOX toxicity. A, Cleaved caspase-3 expression in WT and MT-TG ECTs increased following DOX (0.5 μM for 24 h) and was not decreased in MT overexpression ECTs. B, LDH release in WT and MT-TG ECTs increased following DOX (0.5 μM for 24 h) and was not decreased in MT overexpression ECTs. n = 4 to 8 ECT per group, *$P < .05$ and ** $P < .01$ vs. corresponding Ctrl ECT.

2.4. Histology

ECTs were harvested from the Tissue TrainTM plate on day 7 and the mid-portion of the ECT was washed 3 times in PBS then placed in a Tissue Tek® Cryomold (Torrance, CA) with OCT compound for embedding followed by snap freezing in liquid nitrogen. Individual 5 μm cryostat sections were mounted, fixed in acetone for 5–10 min, washed in 1% Triton-X-100/PBS for 1 h at room temperature, then blocked with 1% Triton-X-100/PBS + 10% FBS for 1 h. ECT sections were stained with mouse anti-cTnT (1:500 dilution; Thermo Fisher Scientific, Fremont, CA). Other sections were mounted using SlowFade™ Gold Antifade Mountant to image DAPI (Thermo Fisher Scientific, Eugene, OR). We randomly select 10 fields per ECT to count double stained cTnT (Red) and DAPI (Blue) positive cells, and the cTnT+/DAPI+ percentage was used to determine the ratio of CM in ECTs [9].

2.5. Protein extraction and western blotting

ECT Western blot assays were performed as previously described [9]. Briefly, ECTs were washed in ice cold PBS and rapidly homogenized in lysis buffer (100 μL/ECT) at 4 °C for 4 h. After centrifugation at 12,000 rpm for 20 min, supernatants containing soluble proteins were measured using Bradford methods. Equal amounts of protein (20 μg) were loaded for analysis. Primary antibodies included cleaved caspase-3, Bax, Bcl-2, CAT, HO-1, Nrf2, NQO-1, p-H2AX, P53, SOD2, and TOP2b (1:1000 dilution; Cell Signaling Technology, Danvers, MA), followed by Anti-rabbit HRP-linked secondary antibody (1:5000 dilution; Cell Signal, Danvers, MA). We report cleaved caspase-3 rather

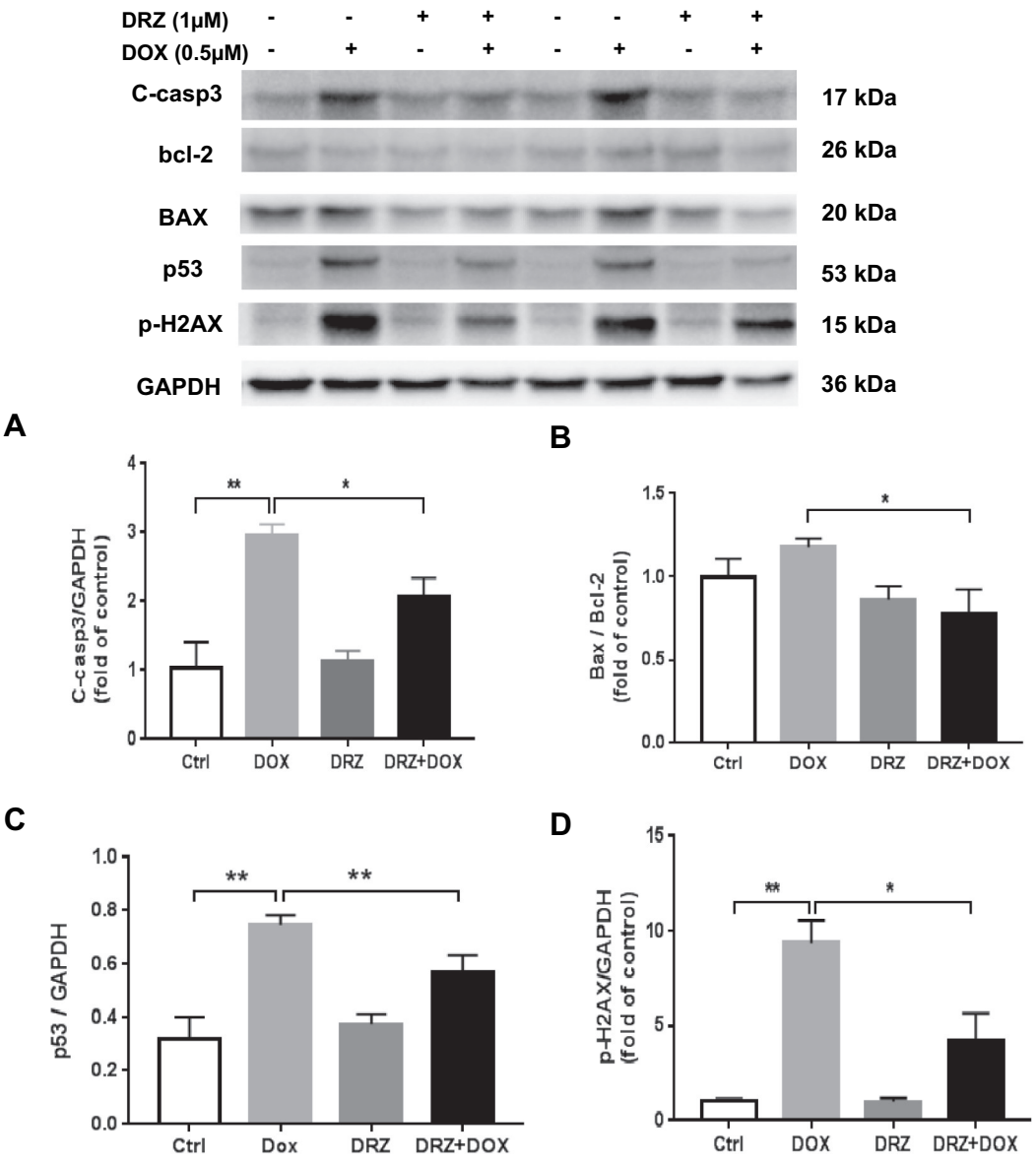

Fig. 5. DRZ pretreatment reduced ECT DOX toxicity. DRZ pretreatment (1 μM for 2 h) reduced A, Cleaved caspase-3; B, Bax/Bcl-2 ratio; C, p53, and D, p-H2AX expression following DOX (0.5 μM for 24 h) treatment. n = 4 ECT per group, *$P < .05$ and ** $P < .01$ vs. corresponding groups.

than total caspase-3 because of the inability to detect both cleaved and total caspase-3 in the same Western blot. MT expression was detected by a modified Western blot protocol as previously described using an MT antibody (1:1000 dilution; Dako, Carpinteria, CA)[46]. Protein expression levels were normalized to GAPDH (1:3000 dilution; Abcam, Cambridge, MA) as an internal control.

2.6. RNA extraction and real-time PCR quantification

RNA extraction and quantitative real time PCR was performed as previously described [9]. GAPDH expression was used as the internal control.

2.7. TdT-mediated dUTP nick-end labeling assay (TUNEL)

We used the DeadEnd™ Colorimetric TUNEL System (Promega, Madison, WI) to determine the proportion of apoptotic cells. Briefly, 5 μm paraffin ECT sections were dewaxed in xylene, and dehydrated in decreasing concentrations of ethanol (100%, 95%, 85%, 70%, 50%). After 4% formaldehyde fixation in PBS, ECT tissues were permeabilized in 20 μg/mL Proteinase K solution, refixed in 4% formaldehyde, and labeled with TdT reaction mix. After mounting with SlowFade™ Gold Antifade Mountant with DAPI (Thermo Fisher Scientific, Eugene, OR), apoptotic cells (green) were detect by fluorescence microscopy. TUNEL positive cells were counted in 15 fields per ECT to determine the TUNEL positive cells/DAPI percentage as an apoptosis ratio.

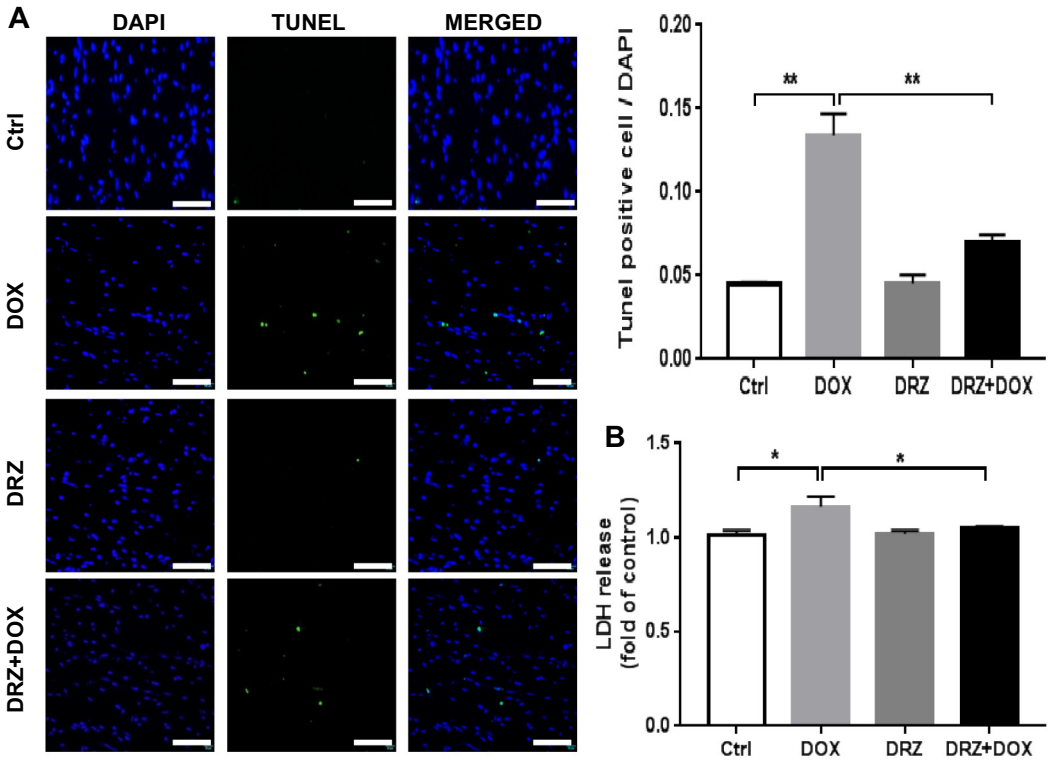

Fig. 6. DRZ pretreatment reduced ECT DOX related cell death measured by terminal transferase dUTP nick end labeling assay (Tunel assay) and LDH release. A, Representative ECT immunofluorescent staining for nuclei (DAPI, blue) and Tunel (green). 40× magnification, Scale bar = 50 μm. DRZ pretreatment (1 μM for 2 h) reduced DOX induced Tunel staining but did not affect the ratio of baseline Tunel positive cells. B, DRZ pretreatment (1 μM for 2 h) reduced DOX induced increase in LDH release but did not affect baseline LDH release. n = 4 ECT per group, $*P < .05$ and $**P < .01$ vs corresponding groups. (For interpretation of the references to colour in this figure legend, the reader is referred to the web version of this article.)

2.8. Lactate dehydrogenase release in culture medium

We used Pierce™ LDH Cytotoxicity Assay Kit (Thermo Fisher Scientific, Rockford, IL) to determine the LDH release into the culture medium [47] as an index of necrotic cell death [48]. Briefly, 50 μL of each sample medium was transferred to a 96-well flat bottom plate in duplicate wells, mixed with 50 μL of Reaction Mixture, then incubated room temperature for 30 min in the dark followed by the addition of 50 μL of Stop Solution to each sample well. Light absorbance at 490 nm and 680 nm was measured using a Molecular Devices SprectraMax (Molecular Devices, Sunnyvale, CA) to quantify signal (490 nm) and noise (680 nm) absorbance.

2.9. Measurement of malondialdehyde levels in ECTs

Malondialdehyde (MDA) levels in ECTs were quantified using a thiobarbituric acid (TBA) reactive species (TBARS) assay [49]. ECT protein was extracted and the protein concentration determined as mentioned above. We combined ECT protein (50 μL), 8.1%SDS (20 μL), 20% Acetic acid (150 μL), and 0.57%TBA (210 μL), and heated at 90 °C for 70 mins followed by ice quenching. After adding ddH2O (100 μL/EP tube), samples were centrifuged at 4000 rpm for 15 mins then read OD at 540 nm (96 plate, 150 μL/well, duplication) using a Molecular Devices SprectraMax (Molecular Devices, Sunnyvale, CA). We then determined the MDA/OD sample/protein ratio for treatment and control groups.

2.10. Statistical analyses

Data are presented as mean ± standard error of the mean (SEM). Statistical differences were determined using two-sided, unpaired Student's *t*-tests or one-way analysis of variance (ANOVA) followed by Tukey's multiple comparisons test. *P* value < .05 was considered statistically significant.

3. Results

3.1. Dose and time-dependent response of ECT DOX induced toxicity

We noted a dose dependent increase in ECT cell death, indexed by increased cleaved caspase-3, after 0.1 to 1.0 μM DOX treatment for 24 h, as well as a time dependent effect of DOX toxicity (Figure 1, 2, 3, 4, 5, 6, 7, 8, 9, 10 and 11A). The threshold DOX dose required to detect increased cleaved caspase-3 expression at 24 h was 0.25 μM, however, a lower dose 0.1 μM DOX increased cleaved caspase-3 expression by 48 h (Fig. 1A). Cumulative LDH release into the culture medium, an additional indicator of cell injury, also showed a time dependent response to DOX treatment (Fig. 1B). Consistent with ECT CM injury, ECT function also showed dose and time dependent DOX toxicity with a progressive inhibition of ECT beating in response to increased DOX dose and duration (Table 1).

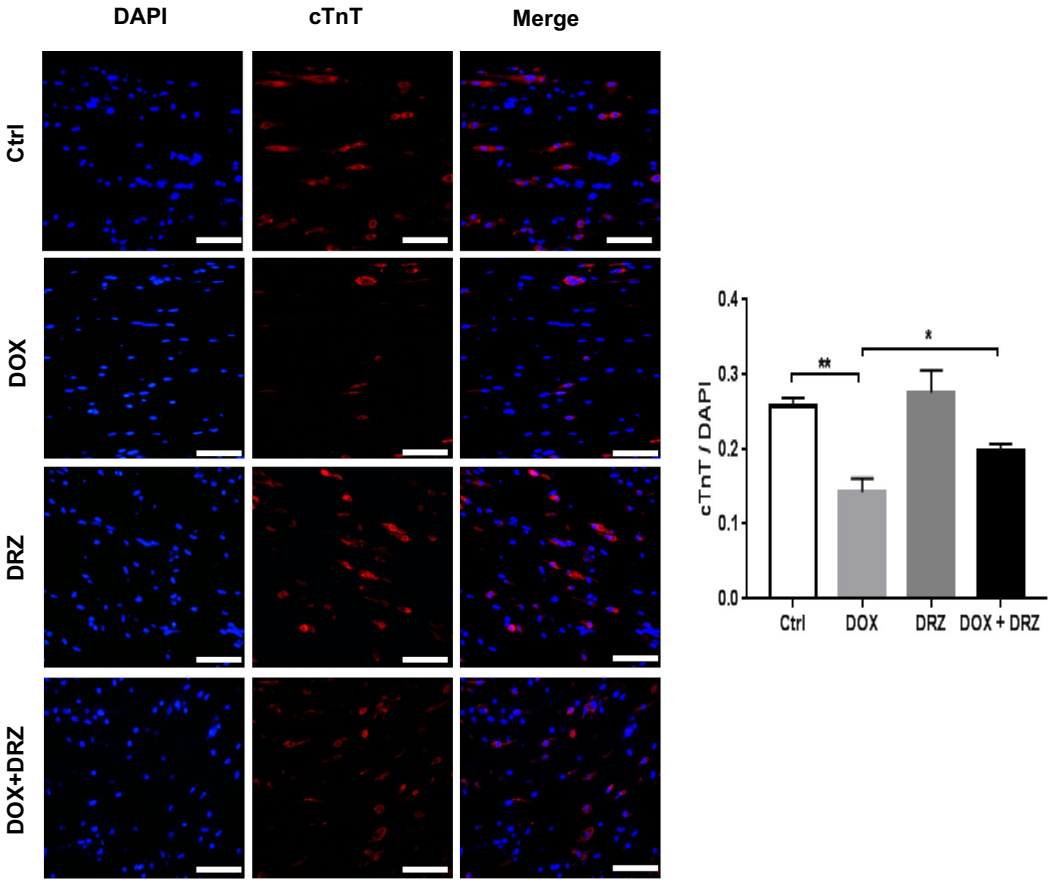

Fig. 7. DRZ pretreatment reduced DOX induced ECT CM loss. Representative ECT CM nuclei stained with DAPI (blue) and sarcomeric cTnT (Red). 40× magnification, Scale bar = 50 μm. DRZ pretreatment (1 μM for 2 h) reduced DOX induced CM loss as measured by the cTnT/DAPI ratio. DRZ pretreatment did not affect the baseline cTnT/DAPI ratio. n = 4 ECT per group, *$P < .05$ and ** $P < .01$ vs. corresponding groups. (For interpretation of the references to colour in this figure legend, the reader is referred to the web version of this article.)

3.2. Zinc induced MT but did not reduce ECT DOX induced toxicity

Since ROS plays an important role in DOX induced cardiotoxicity [37], and Zinc is a potent antioxidant [50] which may protect cardiomyocytes from DOX injury [36] we determined if Zinc could protect against ECT DOX toxicity. As previously described [9], Zinc (50 μM) treatment induced increase ECT MT expression (Fig. 2A). However, Zinc pretreatment did not reduce DOX toxicity as measured by cleaved caspase-3, p53, or LDH release (Fig. 2B, C).

3.3. Cadmium induced MT did not reduce ECT DOX induced toxicity

Although Cd exposure increases ECT MT levels [9], Cd pretreatment (5 μM for 2 h) increased MT (Fig. 3A) but did not reduce ECT DOX toxicity measured by cleaved caspase-3 and p53 levels (Fig. 3B).

3.4. MT overexpression did not reduce ECT DOX induced toxicity

MT overexpression (MT-TG) increases greater ECT MT compared to Cd exposure [9]. Unfortunately, ECT overexpression (Fig. 4A) did not reduce ECT DOX toxicity measured by cleaved caspase-3, p53, or LDH release (Fig. 4B).

3.5. DRZ pretreatment reduced ECT DOX induced toxicity

DRZ pretreatment (1 μM/L for 2 h) reduced ECT DOX toxicity measured by cleaved caspase-3 (Fig. 5A), BAX/Bcl-2 ratio (Fig. 5B), p53 (Fig. 5C), and p-H2AX (Fig. 5D). DRZ pretreatment also reduced DOX toxicity measured by reduced Tunel staining (Fig. 6A), reduced LDH released into the culture media (Fig. 6B), and reduced cardiomyocyte loss measured by the cTnT/DAPI ratio (Fig. 7).

3.6. ROS may not be involved in DRZ-mediated reduced ECT DOX toxicity

In addition to the lack of effect of Zinc or of MT induction on ECT DOX toxicity, we noted that ROS markers, 3-NT (Fig. 8A) and 4-HNE (Fig. 8B) were unchanged by DOX and/or DRZ treatment and there was no change in the expression of Nrf2 or its downstream proteins SOD2, HO-1, CAT, and NQO-1 in response to DOX and/or DRZ treatment (Fig. 9A). MDA, a lipid peroxidation maker, was unchanged by DOX and/or DRZ treatment (Fig. 9B) and pretreatment with the antioxidant drug *N*-acetylcysteine (NAC, 1 mM/L for 2 h) had no effect on cleaved caspase-3 or p53 at baseline or following DOX treatment (Fig. 9C).

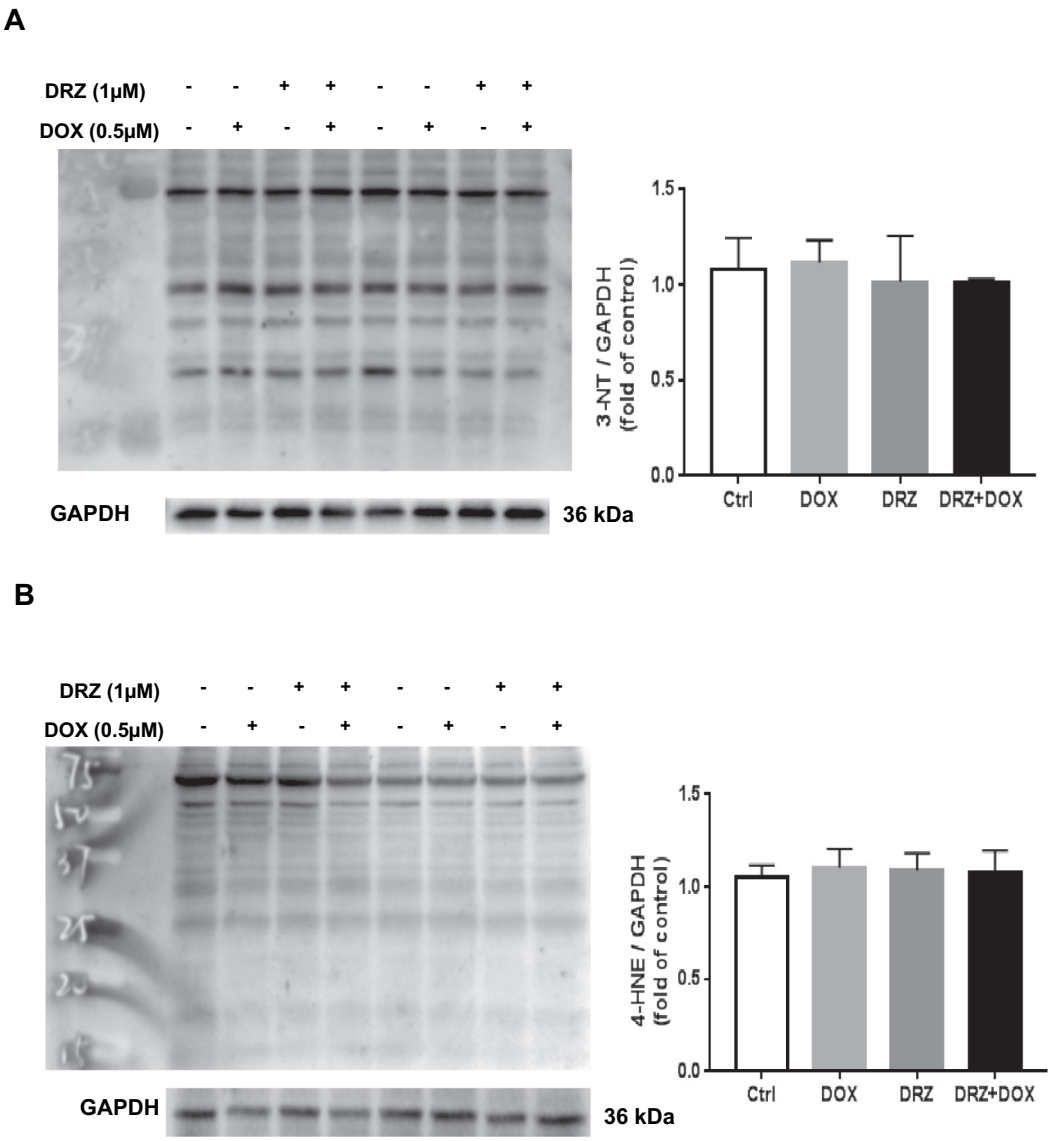

Fig. 8. The ROS markers 3-NT and 4-HNE were unchanged following ECT DOX (0.5 μM for 24 h) and/or DRZ (1 μM for 2 h) treatment. A, 3-NT; B, 4-HNE, n = 3 to 5 ECT per group.

3.7. Reduced TOP2B protein is associated with reduced ECT DOX toxicity

Consistent with previous studies [19,44], we noted that ECT TOP2B protein levels were reduced by DRZ (Fig. 10A) while TOP2B mRNA levels were unchanged (Fig. 10B), consistent with reduced protein stabilization [51].

4. Discussion

The goal of our current study was to test the hypothesis that neonatal murine ECTs can serve as a rapid and robust in vitro model to detect DOX induced cardiotoxicity and to evaluate the response to candidate protective pretreatment strategies. Similar to our success with a neonatal murine ECT model to detect cardiotoxicity from the environmental toxin Cd within 24 h [9], we noted that DOX induced dose and time-dependent ECT cardiotoxicity indicated by increased cleaved caspase-3 expression and LDH release (Fig. 1).

We noted no change in DOX toxicity in response to Zinc or increased MT levels due to Zinc induction or MT-overexpression (Figs. 2–4). MTs are a small cysteine-rich proteins capable of binding 7–12 metal iron per MT molecule and MT functions to efficiently scavenge free radicals as a cellular antioxidant [52] that can reduce diabetes-associated cardiotoxicity [50,53,54]. While increase ROS is recognized to occur in response to DOX cardiotoxicity, and the use of free radical scavengers to decrease DOX cardiotoxicity has been a favorite approach to improve the efficacy of this drug in cancer chemotherapy [55], previous investigators have noted conflicting results that were either favorable related to ROS reduction in DOX toxicity in cell culture [36,38,56,57] or MT-TG mice [58] or negative [59,60]. We did not find evidence for increased ROS (3-NT, 4-HNE, MDA) in ECTs after DOX, similar to the

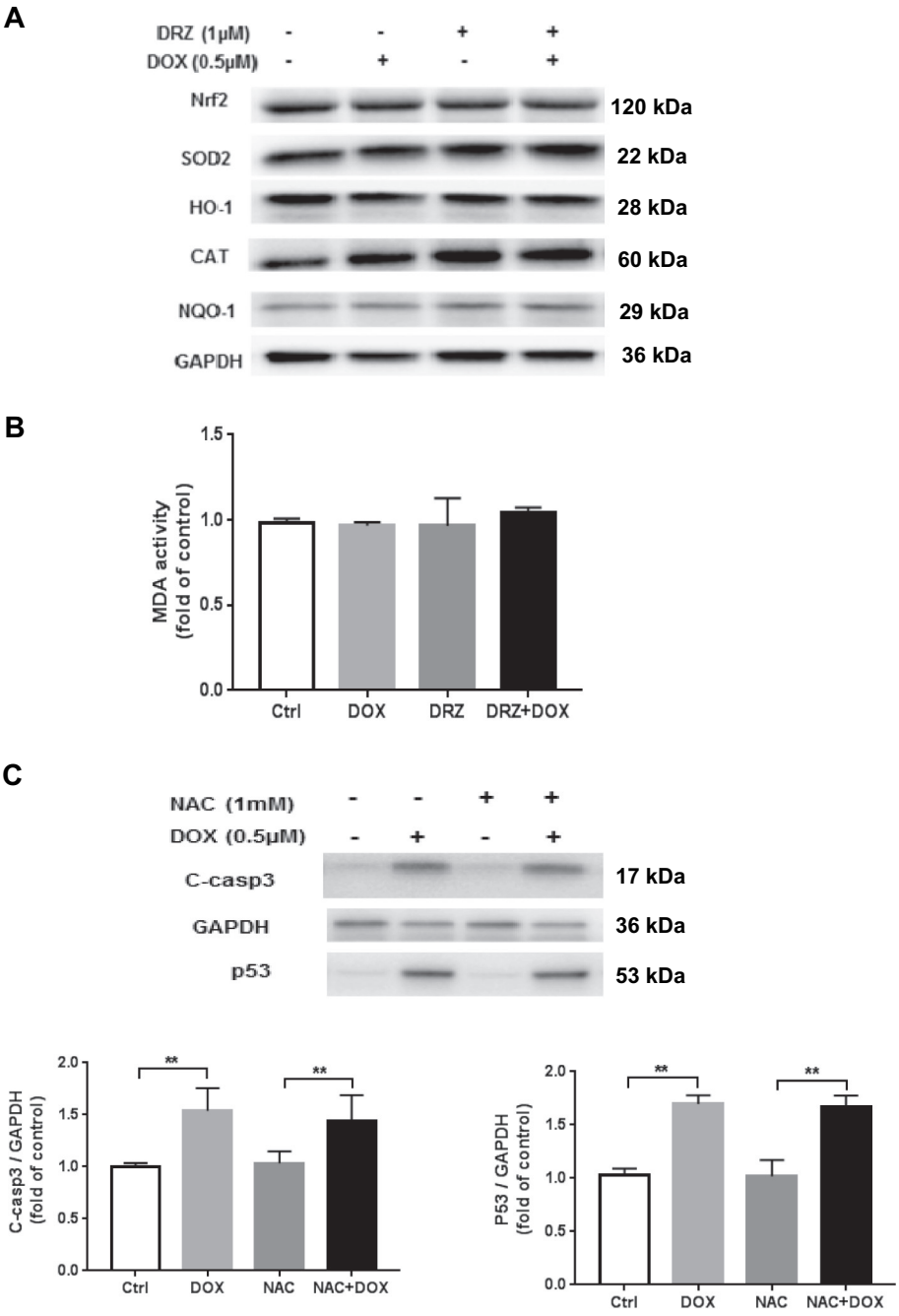

Fig. 9. Multiple anti-oxidant pathway members were unchanged following ECT DOX (0.5 μM for 24 h) and/or DRZ (1 μM for 2 h) treatment. A, Nrf2, SOD2, HO-1, CAT, NQO-1 were unchanged, n = 3 ECT per group; B, MDA activity level was similar in all 4 groups, n = 3 to 5 ECT per group; C, Cleaved caspase-3 and p53 expression was unaffected by NAC, increased after DOX (0.5 μM for 24 h), and was not reduced by NAC pretreatment (1 mM for 2 h), n = 3 ECT per group, $^{**}P < .01$ vs. corresponding Ctrl ECTs.

lack of role for ROS in DOX toxicity in H9C2 cells [61] and the anti-oxidant NAC failed to reduced ECT DOX (Fig. 9C). Futher experiments are required to directly measure ROS within ECTs under various conditions.

Our study confirmed that DRZ provides significant protection from DOX induced ECT cardiotoxicity (Figs. 5–7) that was associated with TOP2B inhibition (Fig. 10). DOX toxicity occurs via stabilizing the covalent topoisomerase II-DNA intermediate (the cleavable complex) which induces DNA double strand breaks. DRZ is the only drug currently approved for prevention against doxorubicin cardiotoxicity [17]. One proposed mechanism for DRZ protection from DOX cardiotoxicity has been attributed to iron chelation by the EDTA-like hydrolysis

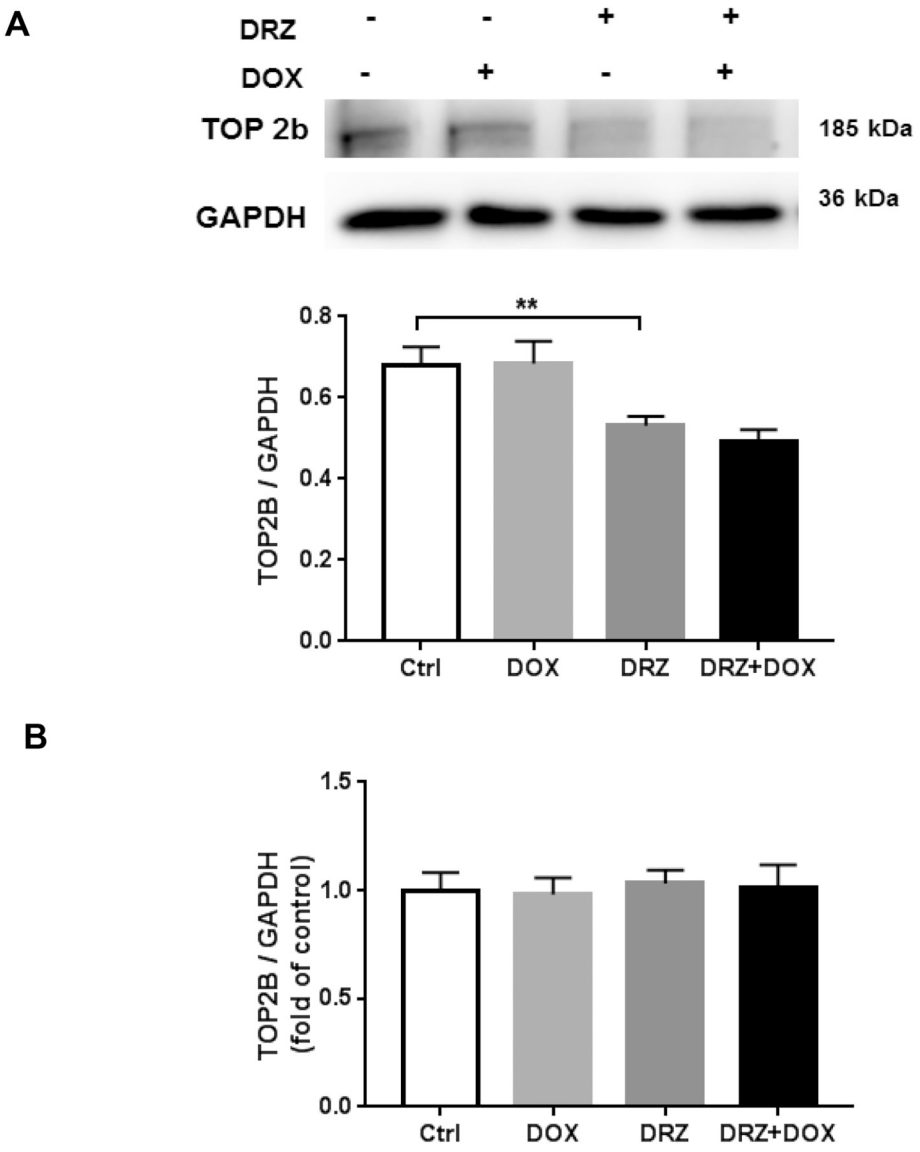

Fig. 10. TOP2B protein, but not mRNA expression was reduced by DRZ pretreatment and neither were affected by DOX. A, TOP2B protein following DRZ (1 μM for 2 h) for 2 h followed by DOX (0.5 μM for 24 h). B, TOP2B mRNA measured by qPCR was similar in all 4 groups. n = 3 to 5 ECT per group, $^{**}P < .01$ vs. Ctrl ECT.

product of DRZ, which decreases ROS [43,62]. However, the cardioprotective role of iron chelation is controversial and the iron chelator ICL670A (Deferasirox) shows no protection against DOX toxicity despite rapid intracellular distribution and efficient iron chelation [63].

Inhibition of TOP2B with subsequently reduced DNA damage is considered to be a primary mechanism for DRZ protection from DOX cardiotoxicity [44]. DRZ reduces the formation of TOP2B-DNA covalent (cleavage) complexes through its stabilization of the ATP-bound closed-clamp conformation of TOP2 which triggers proteasomal degradation of TOP2B. TOP2B depletion results in fewer doxorubicin trapped TOP2B cleavage complexes and reduced DNA damage [51] (Fig. 11). Our data showed that DRZ reduced TOP2B protein levels without changing mRNA levels, consistent with increased protein degradation and reduced DNA damage. Additional ECT studies, including studies using TOB2B knock-out cardiac cells, are warranted to determine the optimal DRZ dose and timing to prevent DOX cardiotoxicity and to validate the role of TOP2B mediated DNA damage and DNA repair pathways.

5. Conclusion

Our data support the paradigm that neonatal murine ECTs can serve an in vitro surrogate model for DOX cardiotoxicity screening and for the evaluation of preventive measures, with DRZ as a representative compound. Further studies are required to determine if DRZ also preserves critical functional aspects of ECT biology including the force-frequency relationship and mechanical-load induced growth. Insights from ECT experiments will need to be translated to more expensive small and large animal preclinical models for further validation.

Author contributions

Juan Zhen: designed and performed experiments, analyzed data, prepared and reviewed manuscript for submission.

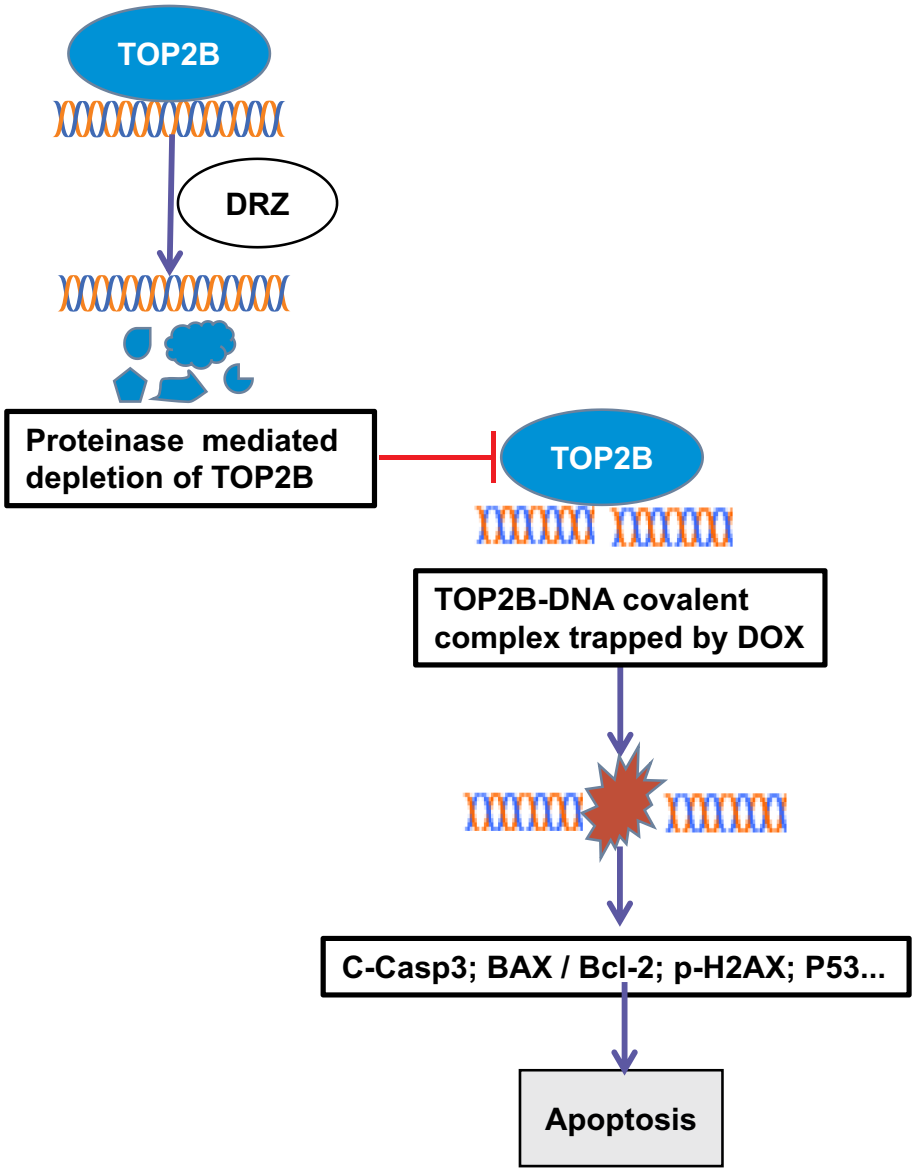

Fig. 11. Possible mechanism of DRZ reduction in DOX ECT toxicity. DRZ binds to DNA-bound TOP2B which triggers proteasomal degradation of TOP2B (TOP2B down-regulation). TOP2B depletion results in fewer doxorubicin trapped TOP2B cleavage complexes, reduced DNA damage, and reduced subsequent cell death via apoptosis. Additional ECT experiments (and in vivo validation) are required related to the role of BAX/Bcl-2 and p-H2AX in DRZ mediated DOX cardioprotection.

Haitao Yu: designed and performed experiments, analyzed data, prepared and reviewed manuscript for submission.

Honglei Ji: designed experiments, prepared and reviewed manuscript for submission.

Lu Cai: designed experiments, prepared and reviewed manuscript for submission.

Jiyan Leng: prepared and reviewed manuscript for submission.

Bradley B. Keller: designed and performed experiments, analyzed data, prepared and reviewed manuscript for submission.

Funding and acknowledgements

This work was supported by the Kosair Charities Pediatric Heart Research Fund to B.K., the U.S-China Pediatric Research Exchange Training Program to L.C. and B.K., the First Hospital of Jilin University Youth Fund (JDYY92018031) to J.Z., the Scientific Technological Development Plan Project in Jilin Province of China (20190701067GH) to J.L., the Jilin Provincial Department of Finance (2018SCZWSZX-005) to J.L., and the National Natural Science Foundation of China (81974027) to H.J. All personnel expenses and partial research-related expenses for Dr. Haitao Yu and Dr. Juan Zhen were provided by Jilin University through a collaborative research agreement between the University of Louisville and Jilin University, Changchun, China. All basic science experiments were completed at the University of Louisville, Louisville, KY, USA.

Declaration of competing interest

The authors declare that there are no scientific or financial conflicts of interest.

Appendix A. Supplementary data

Supplementary data to this article can be found online at https://doi.org/10.1016/j.lfs.2019.117070.

References

[1] A. Hansen, A. Eder, M. Bonstrup, M. Flato, M. Mewe, S. Schaaf, B. Aksehirlioglu, A.P. Schwoerer, J. Uebeler, T. Eschenhagen, Development of a drug screening platform based on engineered heart tissue, Circ. Res. 107 (1) (2010) 35–44.

[2] K.L. Fujimoto, K.C. Clause, L.J. Liu, J.P. Tinney, S. Verma, W.R. Wagner, B.B. Keller, K. Tobita, Engineered fetal cardiac graft preserves its cardiomyocyte proliferation within postinfarcted myocardium and sustains cardiac function, Tissue Eng. A 17 (5–6) (2011) 585–596.

[3] H. Masumoto, T. Nakane, J.P. Tinney, F. Yuan, F. Ye, W.J. Kowalski, K. Minakata, R. Sakata, J.K. Yamashita, B.B. Keller, The myocardial regenerative potential of three-dimensional engineered cardiac tissues composed of multiple human iPS cell-derived cardiovascular cell lineages, Sci. Rep. 6 (2016) 29933.

[4] W.H. Zimmermann, I. Melnychenko, G. Wasmeier, M. Didie, H. Naito, U. Nixdorff, A. Hess, L. Budinsky, K. Brune, B. Michaelis, et al., Engineered heart tissue grafts improve systolic and diastolic function in infarcted rat hearts, Nat. Med. 12 (4) (2006) 452–458.

[5] W.J. de Lange, L.F. Hegge, A.C. Grimes, C.W. Tong, T.M. Brost, R.L. Moss, J.C. Ralphe, Neonatal mouse-derived engineered cardiac tissue: a novel model system for studying genetic heart disease, Circ. Res. 109 (1) (2011) 8–19.

[6] M.N. Hirt, N.A. Sorensen, L.M. Bartholdt, J. Boeddinghaus, S. Schaaf, A. Eder, I. Vollert, A. Stohr, T. Schulze, A. Witten, et al., Increased afterload induces pathological cardiac hypertrophy: a new in vitro model, Basic Res. Cardiol. 107 (6) (2012) 307.

[7] H. Song, P.W. Zandstra, M. Radisic, Engineered heart tissue model of diabetic myocardium, Tissue Engineering. Part A 17 (13–14) (2011) 1869–1878.

[8] A. Stohr, F.W. Friedrich, F. Flenner, B. Geertz, A. Eder, S. Schaaf, M.N. Hirt, J. Uebeler, S. Schlossarek, L. Carrier, et al., Contractile abnormalities and altered drug response in engineered heart tissue from Mybpc3-targeted knock-in mice, J. Mol. Cell. Cardiol. 63 (2013) 189–198.

[9] H. Yu, F. Ye, F. Yuan, L. Cai, H. Ji, B.B. Keller, Neonatal murine engineered cardiac tissue toxicology model: impact of metallothione in overexpression on cadmium-induced injury, Toxicol. Sci. 165 (2) (2018) 499–511.

[10] T. Nakane, H. Masumoto, J.P. Tinney, F. Yuan, W.J. Kowalski, F. Ye, A.J. LeBlanc, R. Sakata, J.K. Yamashita, B.B. Keller, Impact of cell composition and geometry on human induced pluripotent stem cells-derived engineered cardiac tissue, Sci. Rep. 7 (2017) 45641.

[11] K. Ronaldson-Bouchard, S.P. Ma, K. Yeager, T. Chen, L. Song, D. Sirabella, K. Morikawa, D. Teles, M. Yazawa, G. Vunjak-Novakovic, Advanced maturation of human cardiac tissue grown from pluripotent stem cells, Nature. 556 (7700) (2018) 239–243.

[12] Y. Zhao, N. Rafatian, N.T. Feric, B.J. Cox, R. Aschar-Sobbi, E.Y. Wang, P. Aggarwal, B. Zhang, G. Conant, K. Ronaldson-Bouchard, A. Pahnke, S. Protze, J.H. Lee, L. Davenport Huyer, D. Jekic, A. Wickeler, H.E. Naguib, G.M. Keller, G. Vunjak-Novakovic, U. Broeckel, P.H. Backx, M.A. Radisic, Platform for generation of chamber-specific cardiac tissues and disease modeling, Cell. 176 (4) (2019) 913–927.

[13] F. Dos Santos Arruda, F.D. Tome, M.P. Miguel, L.B. de Menezes, P.R.A. Nagib, E.C. Campos, D.F. Soave, M.R.N. Celes, Doxorubicin-induced cardiotoxicity and cardioprotective agents: classic and new players in the game, Current Pharmaceutical Design (2019), https://doi.org/10.2174/1381612825666190312110836.

[14] M. Ivanová, I. Dovinová, L. Okruhlicová, N. Tribulová, P. Simončíková, M. Barteková, J. Vlkovičová, M. Barančík, Chronic cardiotoxicity of doxorubicin involves activation of myocardial and circulating matrix metalloproteinases in rats, Acta Pharmacol. Sin. 33 (4) (2012) 459–469.

[15] Y. Octavia, C.G. Tocchetti, K.L. Gabrielson, S. Janssens, H.J. Crijns, A.L. Moens, Doxorubicin-induced cardiomyopathy: from molecular mechanisms to therapeutic strategies, J. Mol. Cell. Cardiol. 52 (6) (2012) 1213–1225.

[16] J. Zhang, X. Cui, Y. Yan, M. Li, Y. Yang, J. Wang, J. Zhang, Research progress of cardioprotective agents for prevention of anthracycline cardiotoxicity, Am. J. Transl. Res. 8 (7) (2016) 2862–2875.

[17] S. Zhang, X. Liu, T. Bawa-Khalfe, L.S. Lu, Y.L. Lyu, L.F. Liu, E.T. Yeh, Identification of the molecular basis of doxorubicin-induced cardiotoxicity, Nat. Med. 18 (11) (2012) 1639–1642.

[18] T.R. Mancilla, B. Iskra, G.J. Aune, Doxorubicin-induced cardiomyopathy in children, Compr Physiol. 9 (3) (2019) 905–931.

[19] P.W. Burridge, Y.F. Li, E. Matsa, H. Wu, S.G. Ong, A. Sharma, A. Holmström, A.C. Chang, M.J. Coronado, A.D. Ebert, J.W. Knowles, M.L. Telli, R.M. Witteles, H.M. Blau, D. Bernstein, R.B. Altman, J.C. Wu, Human induced pluripotent stem cell-derived cardiomyocytes recapitulate the predilection of breast cancer patients to doxorubicin-induced cardiotoxicity, Nat. Med. 22 (5) (2016) 547–556.

[20] T. Magdy, B.T. Burmeister, P.W. Burridge, Validating the pharmacogenomics of chemotherapy-induced cardiotoxicity: what is missing? Pharmacol. Ther. 168 (2016) 113–125.

[21] E.A. Pinheiro, K.A. Fetterman, P.W. Burridge, hiPSCs in cardio-oncology: deciphering the genomics, Cardiovasc Res. 115 (5) (2019) 935–948.

[22] X.Z. Han, S. Gao, Y.N. Cheng, Y.Z. Sun, W. Liu, L.L. Tang, D.M. Ren, Protective effect of naringenin-7-O-glucoside against oxidative stress induced by doxorubicin in H9c2 cardiomyocytes, Biosci Trends. 6 (1) (2012) 19–25.

[23] L.J. Xu, L. Jin, H. Pan, A.Z. Zhang, G. Wei, P.P. Li, W.Y. Lu, Deferiprone protects the isolated atria from cardiotoxicity induced by doxorubicin, Acta Pharmacol. Sin. 27 (10) (2006) 1333–1339.

[24] S.H. Zhang, W.Q. Wang, J.L. Wang, Protective effect of tetrahydroxystilbene glucoside on cardiotoxicity induced by doxorubicin in vitro and in vivo, Acta Pharmacol. Sin. 30 (11) (2009) 1479–1487.

[25] F. Cai, M.A.F. Luis, X. Lin, M. Wang, L. Cai, C. Cen, E. Biskup, Anthracycline-induced cardiotoxicity in the chemotherapy treatment of breast cancer: preventive strategies and treatment, Mol Clin Oncol. 11 (1) (2019) 15–23.

[26] F. Belmonte, S. Das, P. Sysa-Shah, V. Sivakumaran, B. Stanley, X. Guo, N. Paolocci, M.A. Aon, M. Nagane, P. Kuppusamy, C. Steenbergen, K. Gabrielson, ErbB2 overexpression upregulates antioxidant enzymes, reduces basal levels of reactive oxygen species, and protects against doxorubicin cardiotoxicity, Am. J. Physiol. Heart Circ. Physiol. 309 (8) (2015) H1271–H1280.

[27] K. Saeki, I. Obi, N. Ogiku, M. Shigekawa, T. Imagawa, T. Matsumoto, Doxorubicin directly binds to the cardiac-type ryanodine receptor, Life Sci. 70 (20) (2002) 2377–2389.

[28] E. Gammella, F. Maccarinelli, P. Buratti, S. Recalcati, G. Cairo, The role of iron in anthracycline cardiotoxicity, Front. Pharmacol. 5 (2014) 25.

[29] M.P. Catanzaro, A. Weiner, A. Kaminaris, C. Li, F. Cai, F. Zhao, S. Kobayashi, T. Kobayashi, Y. Huang, H. Sesaki, Q. Liang, Doxorubicin-induced cardiomyocyte death is mediated by unchecked mitochondrial fission and mitophagy, FASEB J. (2019), https://doi.org/10.1096/fj.201802663R.

[30] L.E. Wold, N.S. Aberle 2nd, J. Ren, Doxorubicin induces cardiomyocyte dysfunction via a p38 MAP kinase-dependent oxidative stress mechanism, Cancer Detect. Prev. 29 (3) (2004) 294–299.

[31] A.J. Dirks-Naylor, The role of autophagy in doxorubicin-induced cardiotoxicity, Life Sci. 93 (24) (2013) 913–916 (Review).

[32] S. Shabalala, C.J.F. Muller, J. Louw, R. Johnson, Polyphenols, autophagy and doxorubicin-induced cardiotoxicity, Life Sci. 180 (2017) 160–170.

[33] L. Ponnusamy, P.K. Mahalingaiah, K.P. Singh, Chronic oxidative stress increases resistance to doxorubicin-induced cytotoxicity in renal carcinoma cells potentially through epigenetic mechanism, Mol. Pharmacol. 89 (1) (2016) 27–41.

[34] Y.Y. Zhang, C. Meng, X.M. Zhang, C.H. Yuan, M.D. Wen, Z. Chen, D.C. Dong, Y.H. Gao, C. Liu, Z. Zhang, Ophiopogonin D attenuates doxorubicin-induced autophagic cell death by relieving mitochondrial damage in vitro and in vivo, J. Pharmacol. Exp. Ther. 352 (1) (2015) 166–174.

[35] S. Li, W. Wang, T. Niu, H. Wang, B. Li, Nrf2 deficiency exaggerates doxorubicin-induced cardiotoxicity and cardiac dysfunction, Oxidative Med. Cell. Longev. 2014 (2014) 748524.

[36] L. Jing, L. Li, J. Zhao, J. Zhao, Z. Sun, S. Peng, Zinc-induced metallothionein overexpression prevents doxorubicin toxicity in cardiomyocytes by regulating the peroxiredoxins, Xenobiotica 46 (8) (2016) 715–725.

[37] M. Songbo, H. Lang, C. Xinyong, X. Bin, Z. Ping, S. Liang, Oxidative stress injury in doxorubicin-induced cardiotoxicity, Toxicol. Lett. 307 (2019) 41–48.

[38] G.W. Wang, Y.J. Kang, Inhibition of doxorubicin toxicity in cultured neonatal mouse cardiomyocytes with elevated metallothionein levels, J. Pharmacol. Exp. Ther. 288 (3) (1999) 938–944.

[39] W. Feng, F.W. Benz, J. Cai, W.M. Pierce, Y.J. Kang, Metallothionein disulfides are present in metallothionein-overexpressing transgenic mouse heart and increase under conditions of oxidative stress, J. Biol. Chem. 281 (2) (2006) 681–687.

[40] M.F.R. Zare, K. Rakhshan, N. Aboutaleb, F. Nikbakht, N. Naderi, M. Bakhshesh, Y. Azizi, Apigenin attenuates doxorubicin induced cardiotoxicity via reducing oxidative stress and apoptosis in male rats, *Life Sci.* (2019) 116623, https://doi.org/10.1016/j.lfs.2019.116623.

[41] B.L. Asselin, M. Devidas, L. Chen, V.I. Franco, J. Pullen, M.J. Borowitz, R.E. Hutchison, Y. Ravindranath, S.H. Armenian, B.M. Camitta, S.E. Lipshultz, Cardioprotection and safety of dexrazoxane in patients treated for newly diagnosed T-cell acute lymphoblastic leukemia or advanced-stage lymphoblastic non-Hodgkin lymphoma: a report of the children's oncology group randomized trial pediatric oncology group 9404, J. Clin. Oncol. 34 (8) (2017) 854–862.

[42] P. Reichardt, M.D. Tabone, J. Mora, B. Morland, R.L. Jones, Risk-benefit of dexrazoxane for preventing anthracycline-related cardiotoxicity: re-evaluating the European labeling, Future Oncol. 14 (25) (2018) 2663–2676.

[43] Y. Ichikawa, M. Ghanefar, M. Bayeva, R. Wu, A. Khechaduri, S.V. Naga Prasad, R.K. Mutharasan, T.J. Naik, H. Ardehali, Cardiotoxicity of doxorubicin is mediated through mitochondrial iron accumulation, J. Clin. Invest. 124 (2) (2014) 617–630.

[44] S. Deng, T. Yan, C. Jendrny, A. Nemecek, M. Vincetic, U. Godtel-Armbrust, L. Wojnowski, Dexrazoxane may prevent doxorubicin-induced DNA damage via depleting both topoisomerase II isoforms, BMC Cancer 14 (2014) 842.

[45] V. Vijay, C.L. Moland, T. Han, J.C. Fuscoe, T. Lee, E.H. Herman, G.R. Jenkins, S.M. Lewis, C.A. Cummings, Y. Gao, et al., Early transcriptional changes in cardiac mitochondria during chronic doxorubicin exposure and mitigation by dexrazoxane in mice, Toxicol. Appl. Pharmacol. 295 (2016) 68–84.

[46] J. Wang, Y. Song, L. Elsherif, Z. Song, G. Zhou, S.D. Prabhu, J.T. Saari, L. Cai, Cardiac metallothionein induction plays the major role in the prevention of diabetic cardiomyopathy by zinc supplementation, Circulation 113 (4) (2006) 544–554.

[47] S.R. Adderley, D.J. Fitzgerald, Oxidative damage of cardiomyocytes is limited by extracellular regulated kinases 1/2-mediated induction of cyclooxygenase-2, J Biol Chem 274 (8) (1999) 5038–5046.

[48] F.K. Chan, K. Moriwaki, M.J. De Rosa, Detection of necrosis by release of lactate dehydrogenase activity, Methods Mol. Biol. 979 (2013) 65–70.

[49] T. Bai, X. Hu, Y. Zheng, S. Wang, J. Kong, L. Cai, Resveratrol protects against lipopolysaccharide-induced cardiac dysfunction by enhancing SERCA2a activity through promoting the phospholamban oligomerization, Am. J. Physiol. Heart Circ. Physiol. 311 (4) (2016) H1051–h1062.

[50] M. Jarosz, M. Olbert, G. Wyszogrodzka, K. Mlyniec, T. Librowski, Antioxidant and anti-inflammatory effects of zinc. Zinc-dependent NF-kappaB signaling, Inflammopharmacology 25 (1) (2017) 11–24.

[51] Y.L. Lyu, J.E. Kerrigan, C.P. Lin, A.M. Azarova, Y.C. Tsai, Y. Ban, L.F. Liu, Topoisomerase IIbeta mediated DNA double-strand breaks: implications in

doxorubicin cardiotoxicity and prevention by dexrazoxane, Cancer Res. 67 (18) (2007) 8839–8846.
[52] D. Juarez-Rebollar, C. Rios, C. Nava-Ruiz, M. Mendez-Armenta, Metallothionein in Brain Disorders, Oxidative Med. Cell. Longev. 2017 (2017) 5828056.
[53] D.D. Marreiro, K.J. Cruz, J.B. Morais, J.B. Beserra, J.S. Severo, A.R. de Oliveira, Zinc and oxidative stress: current mechanisms, Antioxidants (Basel, Switzerland) 6 (2) (2017).
[54] Y. Park, J. Zhang, L. Cai, Reappraisal of metallothionein: clinical implications for patients with diabetes mellitus, J. Diabetes. 10 (3) (2018) 213–231.
[55] R.M. Damiani, D.J. Moura, C.M. Viau, R.A. Caceres, J.A.P. Henriques, J. Saffi, Pathways of cardiac toxicity: comparison between chemotherapeutic drugs doxorubicin and mitoxantrone, Arch. Toxicol. 90 (9) (2016) 2063–2076.
[56] M. Satoh, A. Naganuma, N. Imura, Modulation of adriamycin toxicity by tissue-specific induction of metallothionein synthesis in mice, Life Sci. 67 (6) (2000) 627–634.
[57] Y. Wang, X. Mei, J. Yuan, W. Lu, B. Li, D. Xu, Taurine zinc solid dispersions attenuate doxorubicin-induced hepatotoxicity and cardiotoxicity in rats, Toxicol. Appl. Pharmacol. 289 (1) (2015) 1–11.
[58] Y.J. Kang, Z.X. Zhou, G.W. Wang, A. Buridi, J.B. Klein, Suppression by metallothionein of doxorubicin-induced cardiomyocyte apoptosis through inhibition of p38 mitogen-activated protein kinases, J. Biol. Chem. 275 (18) (2000) 13690–13698.
[59] R.A. DiSilvestro, J. Liu, C.D. Klaassen, Transgenic mice overexpressing metallothionein are not resistant to adriamycin cardiotoxicity, Res. Commun. Mol. Pathol. Pharmacol. 93 (2) (1996) 163–170.
[60] K.E. Merten, Y. Jiang, Y.J. Kang, Zinc inhibits doxorubicin-activated calcineurin signal transduction pathway in H9c2 embryonic rat cardiac cells, Exp. Biol. Med. 232 (5) (2007) 682–689.
[61] T. Rharass, A. Gbankoto, C. Canal, G. Kursunluoglu, A. Bijoux, D. Panakova, A.C. Ribou, Oxidative stress does not play a primary role in the toxicity induced with clinical doses of doxorubicin in myocardial H9c2 cells, Mol. Cell. Biochem. 413 (1–2) (2016) 199–215.
[62] L. Yalcintepe, E. Halis, Modulation of iron metabolism by iron chelation regulates intracellular calcium and increases sensitivity to doxorubicin, Bosnian Journal of Basic edical Sciences 16 (1) (2016) 14–20.
[63] B.B. Hasinoff, D. Patel, X. Wu, The oral iron chelator ICL670A (deferasirox) does not protect myocytes against doxorubicin, Free Radic. Biol. Med. 35 (11) (2003) 1469–1479.